Volcano Transition in a Solvable Model of Frustrated Oscillators

Bertrand Ottino-Löffler and Steven H. Strogatz
Center for Applied Mathematics, Cornell University, Ithaca, New York 14853, USA

In 1992, a puzzling transition was discovered in simulations of randomly coupled limit-cycle oscillators. This so-called volcano transition has resisted analysis ever since. It was originally conjectured to mark the emergence of an oscillator glass, but here we show it need not. We introduce and solve a simpler model with a qualitatively identical volcano transition and find that its supercritical state is not glassy. We discuss the implications for the original model and suggest experimental systems in which a volcano transition and oscillator glass may appear.

Large systems of attractively coupled limit-cycle oscillators can show synchronization transitions analogous to ferromagnetic phase transitions [1,2]. These transitions have been observed in chemical systems [3] and are predicted for arrays of lasers [4–6], biological oscillators [1], Josephson junctions [7], and optomechanical systems [8]. The analogy to ferromagnetism led Daido [9,10] to conjecture that, if the purely attractive couplings were replaced by a frustrated mix of attractive and repulsive couplings, oscillator arrays could potentially behave like spin glasses [9–12]. So far, however, only a few counterparts of the phenomena observed in spin glasses have been seen in oscillator arrays [13]. Finding, characterizing, and even defining a true "oscillator glass" remains controversial [9,10,13–20].

The search for oscillator glass began with a natural model: $N \gg 1$ phase oscillators with random symmetric Gaussian couplings as in the Sherrington-Kirkpatrick spin-glass model [21]. Simulations revealed a change in the model's distribution of complex local fields as the variance of the Gaussian couplings was increased. At a critical variance, the distribution switched from being concave down at the origin to concave up, thus forming a volcano-like surface and defining the "volcano" transition [10]. Daido suggested this transition might also signal the onset of an oscillator glass. Further evidence was provided by the numerical observation of slow (algebraic rather than exponential) relaxation from an initially synchronous state to an incoherent state. To explain these results analytically, later studies sought similar phenomena in more tractable models [13,18–20,22], but so far the volcano transition and the glassy state have remained elusive.

In this Letter, we present a model with a solvable volcano transition. It uses a coupling matrix whose rank is controlled by a parameter K. In the low-rank regime $2 \leq K \ll \log_2 N$ the model's dynamics are nonglassy above threshold. Thus, the volcano transition is not indicative of an oscillator glass; in the model studied here, it merely signals

a synchronization transition in the presence of frustration. Unfortunately, our analysis does not extend to the high-rank regime $K = O(N)$ of more direct relevance to Daido's results [10]. For now, that case remains out of reach. Whether a true oscillator glass exists in this or some other regime thus remains an open question.

Following Daido [10], our model consists of coupled phase oscillators. Oscillator j couples with strength J_{jk} to oscillator k via the sine of their phase difference. The governing equations are

$$\dot{\theta}_j = \omega_j + \sum_{k=1}^{N} J_{jk} \sin(\theta_k - \theta_j), \tag{1}$$

for $j = 1, \ldots, N$. Here θ_j denotes the phase of oscillator j and ω_j is its natural frequency, selected at random from a given probability distribution. Instead of the Gaussian frequencies and couplings studied in Ref. [10], for the sake of solvability, we consider Lorentzian-distributed frequencies with density

$$g(\omega) = \frac{1}{\pi(1 + \omega^2)}$$

and define the couplings as follows. Given an even integer $K > 0$ and a coupling scale factor $J \geq 0$, let

$$J_{jk} = \frac{J}{N} \sum_{m=1}^{K} (-1)^m u_m^{(j)} u_m^{(k)}. \tag{2}$$

Here, for each oscillator j, the interaction vector $(u_1^{(j)}, \ldots, u_K^{(j)})$ is a random binary vector of length K with each entry independently being ± 1 with equal probability. Notice that the diagonal of J_{jk} will always be zero (since it is an alternating sum of 1 s), and $J_{jk} = J_{kj}$. In other respects, the entries of the matrix are independent random
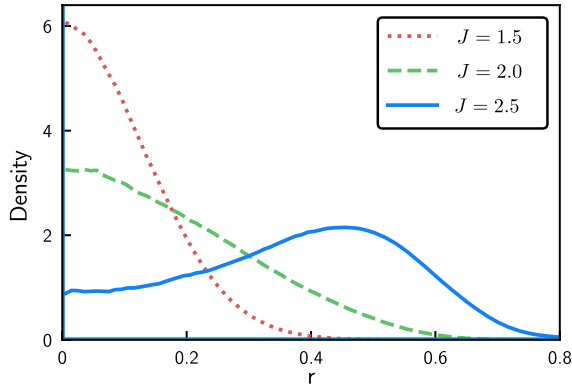
FIG. 1. Radial distribution of local fields. Each curve represents the averaged density over 500 simulations of Eq. (1), using $N = 250$, $K = 4$, fourth-order Runge-Kutta integration with a step size of 0.01, 1000 transient steps, 2000 recorded steps, and uniformly random initial phases.

FIG. 2. Oscillator phase distributions below and above the volcano transition. (a), (b) $J = 1$; (c), (d) $J = 3$. Each panel shows results for simulations of $N = 2000$ and $K = 6$; other parameters as in Fig. 1. (a) Below the volcano transition, the system is incoherent. (b) Density of $\theta_j - \phi_k$, indicating an oscillator's phase relative to that of the local field angle, plotted against the associated coupling strength J_{jk}, normalized and averaged across all k. Darker shades represent higher density. The uniform vertical stripes show that when $J = 1$ the local field has negligible influence on oscillator phases. (c) Above the volcano transition, phase-locked clusters appear. (d) Dark horizontal bands at $\theta_j - \phi_k = 0$ and $\pm\pi$ indicate tendency of oscillators to align or antialign to local field phases, depending on the sign of J_{jk}.

variables (see Supplemental Material [23]). Because of the presence of both positive and negative coupling, this model induces frustration in the oscillator population. In the limit of large N, the parameter K equals the rank of the coupling matrix J_{jk}. Furthermore, if we fix $K \equiv N$ and let N get large, the off-diagonal entries converge to normal random variables with a standard deviation of $J/\sqrt{N}$. So when $K = N \gg 1$, our construction approximates Daido's original Gaussian couplings.

To show numerically that our model has a volcano transition, we compute its complex local fields [10]

$$P_j = r_j e^{i\phi_j} := \sum_{k=1}^{N} J_{jk} e^{i\theta_k},$$

for $j = 1, \ldots, N$. Equation (1) then becomes

$$\dot{\theta}_j = \omega_j + r_j \sin(\phi_j - \theta_j).$$

By keeping track of the P_j over time, we obtain a distribution of their magnitudes r_j for each realization of ω and J_{jk}. Figure 1 averages these distributions over many realizations. As J increases from 1.5 to 2.5, the distribution changes from concave down at the origin to concave up and volcanolike. At a critical J_c, the origin no longer attracts the maximum density. This J_c defines the volcano transition.

Figure 2 illustrates how the individual oscillator phases θ_j behave on either side of the transition. For $J < J_c$, the system is incoherent [Fig. 2(a)]. The phases of the oscillators are uniformly distributed and bear no relation to the coupling strength J_{jk} or the phase ϕ_k of the complex local field [Fig. 2(b)]. In contrast, for $J > J_c$, the oscillators with small $|\omega_j|$ form phase-coherent clusters [Fig. 2(c)]. Figure 2(d) suggests that this partial synchronization is induced by the local fields: if oscillator j couples positively
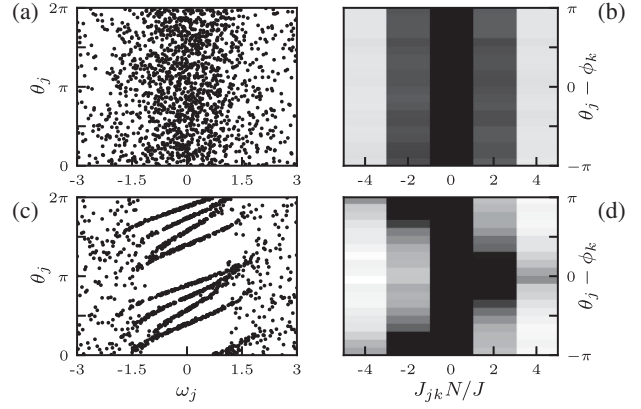
(attractively) to oscillator k, then oscillator j tends to align with the kth local field, whereas if they are negatively (repulsively) coupled, then oscillator j tends to antialign with the local field. In some realizations, we have also observed clustering at phase differences other than zero and π, for moderate values of J_{jk}.

Turning now to the analytical results, we examine Eqs. (1) and (2) in the continuum limit $N \to \infty$ with K held fixed. Using an Eulerian description, we replace our discrete system of oscillators with a continuous fluid moving around the unit circle. Its state is described by a density $f(\theta, \omega, u, t)$ of oscillators with phase θ, natural frequency ω, and interaction vector u. In this framework, the dynamics are given by a continuity equation $f_t + (f\nu)_\theta = 0$, where the subscripts denote partial differentiation, ν represents the velocity field on the circle given by the continuum limit of Eq. (1),

$$\nu(\theta, \omega, u, t) = \omega + \langle J(u, u') \sin(\theta' - \theta) \rangle, \qquad (3)$$

and $\langle \cdot \rangle$ denotes integration using the time-dependent measure $f(\theta', \omega', u', t) d\theta' g(\omega') d\omega' \rho(u') du'$. The coupling term $J(u, u')$ in Eq. (3) plays the role of J_{jk} in Eq. (2). It is given by

$$J(u, u') := J \sum_{m=1}^{K} (-1)^m u_m u'_m.$$

As before, u and u' are random interaction vectors of length K, all of whose entries are ± 1 with probability $1/2$ each. Thus, the probability of any particular vector is 2^{-K}. The associated term in the measure is $\rho(u') = 2^{-K}\sum_v \delta(u' - v)$, where the sum runs over all the equally likely $v \in \{\pm 1\}^K$. Similarly, the continuum limit of the local field is

$$P(u, t) = \langle J(u, u')e^{i\theta'}\rangle.$$

Inserting P in Eq. (3) gives

$$\nu(\theta, \omega, u, t) = \omega + \frac{1}{2i}[e^{-i\theta}P(u, t) - \text{c.c.}].$$

Having derived the continuum model, we reduce it with the Ott-Antonsen ansatz [24–27], a technique that yields the exact long-term dynamics of Kuramoto oscillator models with sinusoidal coupling and Lorentzian frequencies. Following the standard procedure, we seek solutions of the form

$$f(\theta, \omega, u, t) = \frac{1}{2\pi}\left(1 + \sum_{n=1}^{\infty} \alpha(\omega, u, t)^n e^{in\theta} + \text{c.c.}\right),$$

and define $a(u, t) := \alpha(-i, u, t)$. We find [23]

$$\dot{a}(u, t) = -a(u, t) + \frac{P^*(u, t) - a(u, t)^2 P(u, t)}{2}, \quad (4)$$

where

$$P(u, t) = \int J(u, u')a^*(u', t)\rho(u')du'$$

$$= \frac{J}{2^K}\sum_{u'}\sum_{m=1}^{K}(-1)^m u_m u'_m a^*(u', t)$$

Finally, by replacing P in Eq. (4) with this sum, we get a closed set of 2^K ordinary differential equations for the $a(u, t)$, one for each possible choice of u.

Equation (4) has rich dynamics, but for our purposes, it suffices to analyze the stability of its trivial fixed point, $a(u, t) = 0$ for all u and t, because this state corresponds to the incoherent state of Eq. (1). The volcano transition occurs precisely when this state goes unstable. Thus, to calculate J_c, we linearize Eq. (4) about $a \equiv 0$ and determine when one of its eigenvalues is zero. The Jacobian is

$$-I + \frac{J}{2^{K+1}}A. \quad (5)$$

Here I is the $2^K \times 2^K$ identity matrix and

$$A_{uv} = \sum_{m=1}^{K}(-1)^m u_m v_m,$$

where the entries of A have been conveniently indexed by binary strings $u, v \in \{\pm 1\}^K$. The eigenvalues of A can be found explicitly (see Supplemental Material [23]). To do so, we write down the eigenvectors (which we guessed by generalizing from small examples) and then read off the eigenvalues. For each integer $1 \leq n \leq K$ and each binary string $v \in \{\pm 1\}^K$, define a vector $\zeta^{(n)} \in \mathbb{R}^{2^K}$ whose vth entry is $\zeta_v^{(n)} = v_n$. One can check that the set of all K such vectors is orthogonal and, by using the evenness of K, that $A\zeta^{(n)} = (-1)^n 2^K \zeta^{(n)}$. Moreover, given any η perpendicular to all the $\zeta^{(n)}$, one finds $A\eta = 0$. Therefore, A has exactly three distinct eigenvalues: $+2^K$ with multiplicity $K/2$, -2^K with multiplicity $K/2$, and zero with multiplicity $2^K - K$. Consequently, the Jacobian (5) has three distinct eigenvalues, with the largest always being $-1 + J/2$. The conclusion is that the incoherent state for the continuum model loses stability at

$$J_c = 2. \quad (6)$$

This result holds for *any* even value of K.

The next question is whether $J_c = 2$ gives a good approximation to J_c when N is finite. To anticipate the answer, recall that the continuum model reduces to the 2^K-dimensional system (4). For the finite-N system (1) to have any chance of behaving like a continuous fluid of oscillators, we need it to have many oscillators per u and hence to have $N \gg 2^K$.

To test these ideas, we simulate the finite-N system and estimate J_c carefully. To pinpoint the volcano transition, we first compute the one-dimensional (1D) distribution of local field magnitudes $r_j \geq 0$ and fit it to the sum of two normal distributions, with one centered at μ and the other at $-\mu$, and both with variance σ^2. In other words, we approximate the 1D density of local field magnitudes by

$$h(r) = \frac{2}{\sqrt{2\pi\sigma^2}}\exp\left(\frac{-\mu^2 - r^2}{2\sigma^2}\right)\cosh\left(\frac{\mu r}{\sigma^2}\right),$$

for $r \geq 0$. To obtain the full 2D distribution of the P_j's, we impose azimuthal symmetry by rotating and rescaling the 1D density above.

The functional form of $h(r)$ allows us to identify its convexity at the origin. It is concave down when $\gamma := \mu^2/\sigma^2 < 1$ and concave up when $\gamma > 1$. To measure γ numerically, we use the method of moments on the 2D distribution and find [23] that the product of the first and negative first moments is

$$M_{+1}M_{-1} = \frac{\pi}{2}\frac{1 + \gamma}{[e^{-\gamma/2} + \sqrt{\pi\gamma/2}\,\text{Erf}(\sqrt{\gamma/2})]^2}.$$

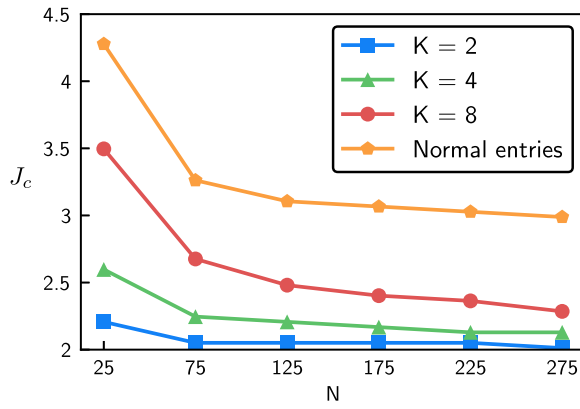The left-hand side can be numerically estimated by aggregating moments from multiple simulations, along

FIG. 3. Critical value J_c versus N and K. Each value of J_c was estimated by using a bisection method on the value of $M_{+1}M_{-1}$ to achieve an accuracy of $\lesssim 0.02$. For each J, we sample J_{jk} at least 100 times, simulate Eq. (1), evaluate $M_{+1}M_{-1}$, and keep track of the running standard deviation of these products. If the current value of $M_{+1}M_{-1}$ is more than 1.5 standard deviations from 1.4694, the bisection continues; otherwise, further simulations are run, up to a maximum of 10^5 simulations. Each simulation consists of 1000 transient steps followed by 2000 recorded steps of a fourth-order Runge-Kutta integration, with a step size of 0.01, with initial phases all set to zero.

FIG. 4. Log-log plot for the decay of the order parameter $Z(t)$. Each curve is the average of 750 numerical integrations of Eq. (1) for $N = 5000$ oscillators starting from the in-phase state ($\theta_j = 0$ for all j) and run for 1000 steps with a step size of 0.01. Solid curves show coupled systems with $J = 10$; dashed curves show uncoupled systems with $J = 0$ for which the order parameter decays exponentially: $Z(t) = e^{-t}$. (a) Low-rank regime: $K \ll \log_2(N)$. For $K = 2$, $Z(t)$ decays exponentially down to the noise floor. Exponential decay is expected in this regime because the dynamics of Eq. (1) are well approximated by the low-dimensional system (4). (b) High-rank regime: $K = N = 5000$. When $K = O(N)$ and $J > J_c$, the relaxation of Z slows markedly, resembling the algebraic decay in glass.

with an appropriate estimate of an error on its total. The right-hand side can be proven to imply that $h(r)$ is concave down at the origin (and therefore $J < J_c$) if and only if $M_{+1}M_{-1} \gtrsim 1.4694$. Thus, by measuring these two moments, we can use a bisection algorithm to zero in on J_c.

Figure 3 shows that, when K is small, $J_c = 2$ becomes an increasingly good estimate as N gets large. For comparison, we also computed J_c for a Gaussian coupling model in which J_{jk} is a random symmetric matrix with normally distributed entries having mean zero and variance J^2/N. As noted earlier, our coupling matrix (2) converges to such a Gaussian matrix when $K = N \gg 1$, but our analytical approach does not extend to this large-K regime. So although the value of J_c for Gaussian coupling decreases as N gets large, we cannot predict whether J_c asymptotically approaches two or not.

A proposed signature feature of oscillator glasses [10,13,13–16] is nonexponential relaxation of the order parameter

$$Z(t) := \sum_{k=1}^{N} e^{i\theta_k(t)}.$$

Figure 4 plots the decay of the order parameter for our model. In the low-rank regime $K \ll \log_2 N$ to which our continuum theory applies, Fig. 4(a) shows that Z decays exponentially fast. This is to be expected, given that the dynamics reduce to a low-dimensional set of ordinary differential equations (4) in this regime. So the dynamics are not glassy here, even above the volcano transition.
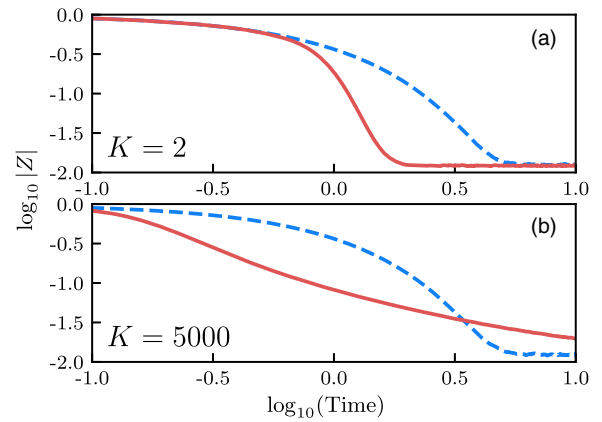
However, outside the low-rank regime, there is some indication that the model can exhibit a glassy state. Figure 4(b) shows that, when $K = N \gg 1$, the order parameter $Z(t)$ decays roughly algebraically for sufficiently large J. This finding aligns with results from Daido's Gaussian coupling model, which has been claimed (controversially) to have algebraic decay [10,14–16]. Understanding the nature of this decay, in both our model and Daido's, remains an open problem. Other aspects of the relationship between the two models need further investigation. Our model has tunable rank, while Daido's model always has full rank. At low rank, the volcano transition in our model produces conspicuous phase clusters, which never occur in Daido's high-rank model. In the high-K regime of our model, a glassy state seems to occur [23], much like that seen in Daido's model. So, presumably, our model has a second transition. Its existence, nature, and connection to Daido's transition remain unclear.

An important future direction is the search for oscillator glasses in the lab and in nature. One promising experimental setup is an array of photosensitive chemical oscillators coupled through a programmable spatial light modulator, as used to create spiral wave chimeras [28]. But we speculate that oscillator glasses may already exist in nature. Given that they would not show any obvious macroscopic signatures, such as collective rhythmicity, they may have escaped notice. There may even be a functional benefit to enforcing incoherence in certain

situations. For instance, although snakes shed their skin in a synchronized molt, humans do not. Perhaps, in cases like this, evolution has selected for glassy states to prevent pathological synchrony.

[1] A. T. Winfree, J. Theor. Biol. **16**, 15 (1967).

[2] Y. Kuramoto, *Chemical Oscillations, Waves, and Turbulence* (Springer, New York, 1984).

[3] I. Z. Kiss, Y. Zhai, and J. L. Hudson, Science **296**, 1676 (2002).

[4] L. Fabiny, P. Colet, R. Roy, and D. Lenstra, Phys. Rev. A **47**, 4287 (1993).

[5] G. Kozyreff, A. G. Vladimirov, and P. Mandel, Phys. Rev. Lett. **85**, 3809 (2000).

[6] R. A. Oliva and S. H. Strogatz, Int. J. Bifurcation Chaos Appl. Sci. Eng. **11**, 2359 (2001).

[7] K. Wiesenfeld, P. Colet, and S. H. Strogatz, Phys. Rev. Lett. **76**, 404 (1996).

[8] G. Heinrich, M. Ludwig, J. Qian, B. Kubala, and F. Marquardt, Phys. Rev. Lett. **107**, 043603 (2011).

[9] H. Daido, Prog. Theor. Phys. **77**, 622 (1987).

[10] H. Daido, Phys. Rev. Lett. **68**, 1073 (1992).

[11] K. H. Fischer and J. A. Hertz, *Spin Glasses* (Cambridge University Press, Cambridge, England, 1993).

[12] T. Castellani and A. Cavagna, J. Stat. Mech. (2005), P05012.

[13] D. Iatsenko, P. V. McClintock, and A. Stefanovska, Nat. Commun. **5**, 4118 (2014).

[14] J. C. Stiller and G. Radons, Phys. Rev. E **58**, 1789 (1998).

[15] H. Daido, Phys. Rev. E **61**, 2145 (2000).

[16] J. C. Stiller and G. Radons, Phys. Rev. E **61**, 2148 (2000).

[17] D. H. Zanette, Europhys. Lett. **72**, 190 (2005).

[18] H. Hong and S. H. Strogatz, Phys. Rev. Lett. **106**, 054102 (2011).

[19] H. Hong and S. H. Strogatz, Phys. Rev. E **84**, 046202 (2011).

[20] H. Hong and S. H. Strogatz, Phys. Rev. E **85**, 056210 (2012).

[21] D. Sherrington and S. Kirkpatrick, Phys. Rev. Lett. **35**, 1792 (1975).

[22] I. M. Kloumann, I. M. Lizarraga, and S. H. Strogatz, Phys. Rev. E **89**, 012904 (2014).

[23] See Supplemental Material at http://link.aps.org/supplemental/10.1103/PhysRevLett.120.264102 for details of mathematical derivations and additional simulations.

[24] E. Ott and T. M. Antonsen, Chaos **18**, 037113 (2008).

[25] E. Ott and T. M. Antonsen, Chaos **19**, 023117 (2009).

[26] A. Pikovsky and M. Rosenblum, Phys. Rev. Lett. **101**, 264103 (2008).

[27] A. Pikovsky and M. Rosenblum, Chaos **25**, 097616 (2015).

[28] J. F. Totz, J. Rode, M. R. Tinsley, K. Showalter, and H. Engel, Nat. Phys. **14**, 282 (2018).